Diffusion Coefficients of Actinide and Lanthanide Ions in Molten Li_2BeF_4

Hirotake Moriyama,*,† Kimikazu Moritani, and Yasuhiko Ito

Department of Nuclear Engineering, Kyoto University, Yoshida, Sakyo-ku, Kyoto 606-01, Japan

Diffusion coefficients of actinide and lanthanide ions in molten Li_2BeF_4 were measured in the temperature range from 813 to 1023 K by a capillary method. The diffusion coefficients of both ions are unusually high, considering the high viscosity of the liquids. The dependence of the diffusion coefficients on temperature and ionic charge are discussed in terms of the theories of Stokes and Einstein.

Introduction

In the conceptual design of molten salt breeder reactors (MSBR) developed at ORNL (*1*), molten fluoride mixtures are used as the fuel carrier and coolant. The fuel salt must be reprocessed continuously in order to meet a high breeding ratio. The main functions of the reprocessing are to isolate ^{233}Pa from the neutron flux and to remove the fission product lanthanides having high neutron absorption cross sections. The processing method involves the reductive extraction of these components from the fuel salt into liquid bismuth solutions in a two phase contacting system.

Extensive studies have been performed on the thermodynamics of reductive extraction (*2–5*), but little is known about the kinetics. Following our previous study of the extraction rate of some typical elements (*6*), the present study deals with the diffusivity of these elements in molten Li_2BeF_4. The temperature dependences of the diffusion coefficients of actinide and lanthanide ions in molten Li_2BeF_4 are measured, and discussed in terms of theories of diffusion.

Experimental Section

Diffusion coefficients were measured by a capillary method (*7, 8*). All the chemicals were of reagent grade obtained from Nacalai Tesque, Inc. In the preliminary dehydration, known amounts of LiF and BeF_2 were put into a graphite crucible and dried by evacuating at 500 K for 1 day. After the dehydration, the salt mixture of Li_2BeF_4 was prepared by melting the components. The radioactive tracers ^{97}Zr, ^{140}La, ^{143}Ce, $^{152m1}Eu$, ^{233}Pa, and ^{239}Np were produced by neutron irradiation of Zr, La, Ce, Eu, Th, and U metals, respectively. Under an inert gas atmosphere, these metals were dissolved in the molten Li_2BeF_4 which was in contact with a small amount of Bi–Li alloy. In a similar system, it has already been found that the radioactive tracers in the salt phase are present as $^{97}Zr^{4+}$, $^{140}La^{3+}$, $^{143}Ce^{3+}$, $^{152m1}Eu^{2+}$, $^{233}Pa^{4+}$, and $^{239}Np^{3+}$ (*2–5*).

A quartz capillary had an i.d. of 0.5 mm and a length of about 50 mm. The open end of the air-evacuated capillary was immersed into the molten Li_2BeF_4 containing the radioactive tracers in order to allow the liquid to rise up. The capillary filled with the molten Li_2BeF_4 was then immersed into pure molten Li_2BeF_4. The temperature of the system was controlled within ±0.5 K with a voltage stabilizer manufactured by Eikoh Electric, Ltd. After a known time, the capillary was removed, allowed to cool, and cut into several sections. The length of each section was from 0.2 to 5.0 mm and measured with a precision of 0.05 mm. The concentration profile of each radioactive tracer was determined by a direct γ-ray spectrometry. The γ-rays of 743 keV (^{97}Zr), 1596 keV (^{140}La), 293 keV (^{143}Ce), 964 keV ($^{152m1}Eu$), 311 keV (^{233}Pa), and 277 keV (^{239}Np) were measured by a high purity germanium detector, EG & G ORTEC.

In the case of the capillary method, thermal convection can be an important source of uncertainty. The effect of thermal convection has been determined for T^+ in molten Li_2BeF_4 (*8*). No significant differences were observed for the capillaries of 0.3 and 0.5 mm, and it was concluded that thermal convection was not an important source of uncertainty. In the present measurement, the uncertainty of the diffusion coefficient is estimated to be ±20% at most, which mostly comes from the statistics of radiation counting.

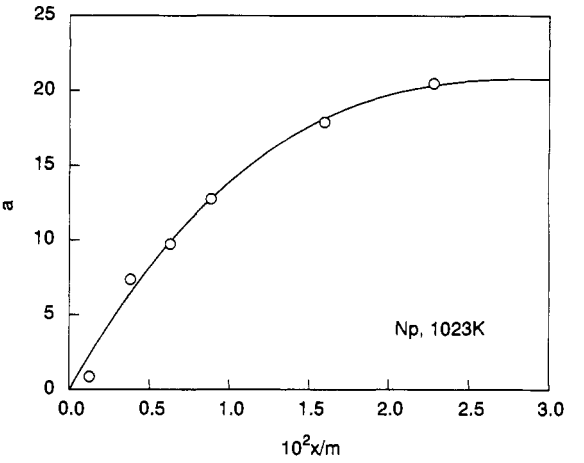

Figure 1. Radioactivity of $^{239}Np^{3+}$, a, at 1023 K as a function of distance. The curve represents the least-squares fit of the data to eq 1.

Results and Discussion

Evaluation of Diffusion Coefficient. Figure 1 shows a typical plot of the concentration of $^{239}Np^{3+}$ at 1023 K. Similar plots were obtained for all the radioactive tracers. The variation of concentration with distance was fitted by

$$c_x = c_0 \,\mathrm{erf}[x/2(Dt)^{1/2}] \qquad (1)$$

where c_x denotes the concentration at a distance x from the open edge of the capillary, c_0 the initial concentration, D the diffusion coefficient, and t the diffusion time. The diffusion coefficient of each ion was determined by a least-squares fit to eq 1. Table 1 summarizes the obtained diffusion coefficients.

† Present address: Research Reactor Institute, Kyoto University, Kumatori-cho, Sennan-gun, Osaka 590-04, Japan.

0021-9568/94/1739-0147$04.50/0

Table 1. Diffusion Coefficients of Some Typical Ions in Molten Li_2BeF_4

ion	T/K	$D^a/(m^2\ s^{-1})$	$c^b/(m^2\ s^{-1}\ K^{-1})$
Np^{3+}	813	2.2×10^{-9}	$(5.7 \pm 0.2) \times 10^{-10}$
	853	3.0×10^{-9}	
	873	3.6×10^{-9}	
	943	5.5×10^{-9}	
	983	7.0×10^{-9}	
	1023	1.0×10^{-8}	
Pa^{4+}	813	1.6×10^{-9}	$(4.7 \pm 0.4) \times 10^{-10}$
	853	2.5×10^{-9}	
	983	6.0×10^{-9}	
	1023	9.0×10^{-9}	
Eu^{2+}	873	4.5×10^{-9}	$(6.9 \pm 0.2) \times 10^{-10}$
	943	7.0×10^{-9}	
	983	8.0×10^{-9}	
	1023	1.1×10^{-8}	
Ce^{3+}	813	2.0×10^{-9}	$(5.2 \pm 0.2) \times 10^{-10}$
	853	2.7×10^{-9}	
	873	3.6×10^{-9}	
	943	5.9×10^{-9}	
	983	6.0×10^{-9}	
La^{3+}	813	2.4×10^{-9}	$(5.8 \pm 0.2) \times 10^{-10}$
	853	3.2×10^{-9}	
	873	3.6×10^{-9}	
	943	5.5×10^{-9}	
	983	6.8×10^{-9}	
	1023	1.0×10^{-8}	
Zr^{4+}	873	2.0×10^{-9}	$(3.2 \pm 0.1) \times 10^{-10}$
	943	3.0×10^{-9}	
	983	4.2×10^{-9}	

[a] The uncertainty of diffusion coefficients is estimated to be ±20% at most. [b] Constant in eq 4.

Temperature Dependence. In Figure 2, the diffusion coefficients are plotted as a function of inverse temperature and compared with literature results for Li^+ (*7*) and T^+ (*8*). Similar temperature dependences are found for all the ions including Li^+ and T^+.

The temperature dependence was analyzed with the Stokes–Einstein equation:

$$D = kT/\alpha\mu r \tag{2}$$

where k is the Boltzmann constant, T the temperature, α a constant, μ the solvent viscosity, and r the effective radius of the diffusing species. The constant α in eq 1 is known to have values in the range $4\pi \leq \alpha \leq 6\pi$ (*9*). For molten nitrates, an α value of 4.6π has been obtained from the analysis of a large amount of cation diffusion–viscosity results (*10*). Similar values have also been obtained for molten halides (*11*), and it is concluded that the Stokes–Einstein equation gives a remarkably good correlation between the diffusion coefficient and viscosity for molten salts (*12*).

The viscosity of molten Li_2BeF_4 as a function of temperature (*13*) can be represented by

$$\mu/(\text{mPa·s}) = 7.4 \times 10^{-4} e^{\{4300/(T/\text{K})\}} \tag{3}$$

By combining eqs 2 and 3, we obtain

$$D = cTe^{\{-4300/(T/\text{K})\}} \tag{4}$$

where c is a constant. The broken curve in Figure 2 represents the least-squares fit of the experimental results of Zr^{4+} to eq 4. The agreement is good, and the temperature dependences are well interpreted by the Stokes–Einstein equation. The obtained c values are given in Table 1.

Although a reasonable agreement is obtained for the temperature dependences, an important disagreement between the observation and theory is found for the effective radius of the diffusing species. By taking the α value of 4.6π for molten nitrates (*9*), the effective radius of the Zr^{4+} species is evaluated from the present data to be 0.4×10^{-10} m. This

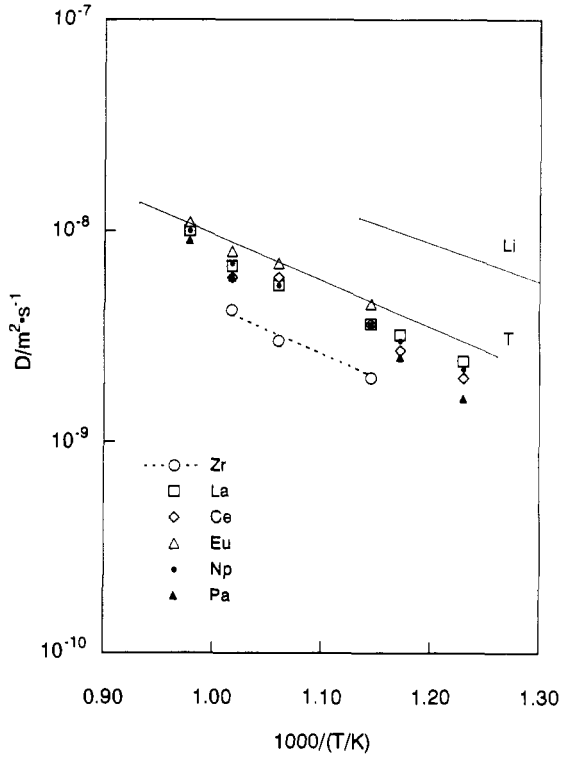

Figure 2. Arrhenius plots of diffusion coefficents of typical ions in molten Li_2BeF_4. The solid curves are taken from the literature for Li^+ (*7*) and T^+ (*8*). The broken curve represents the least-squares fit of the Zr^{4+} data to eq 4, the Stokes–Einstein equation. See the text for details.

value is small compared with the ionic radius of 0.81×10^{-10} m for Zr^{4+}. Similar disagreements are also found for the other elements.

A possible explanation may be given by considering the microscopic structure of molten Li_2BeF_4. The viscosity of molten Li_2BeF_4 is known to be high compared with those of ordinary molten salts due to the glassy structure of BeF_2. Although the glassy structure of BeF_2 is decreased with the increasing fraction of LiF in the mixtures of LiF and BeF_2, a considerable fraction of the polymeric species $Be_mF_n^{2m-n}$ is expected even at the composition of Li_2BeF_4 (*14*). Hence, the microscopic structure of the solvent is no longer homogeneous, and some preferential paths may be present for the diffusing species. The viscosity values we have employed in the evaluation of the effective radius have been measured by means of a steady-state method, which does not account for the local values of viscosity in nonhomogeneous systems. Thus, the discrepancy we have observed is probably due to a difference of the local viscosity in comparison with the measured viscosity. For practical applications with molten Li_2BeF_4, this finding is important because rapid kinetics is expected in spite of the high viscosity of the solvent.

Ionic Charge Dependence. Figure 3 shows the diffusion coefficient as a function of the inverse ionic charge. The diffusion coefficient at 873 K was interpolated by eq 4 from the results in Table 1, and the ionic charge was determined on the basis of experimental observations (*2–5*). In general, the diffusivity decreases with the increasing ionic charge.

The ionic charge dependence of the diffusion coefficient is expressed by the Nernst–Einstein equation

$$D = kTu/ze \tag{5}$$

where u is the ionic mobility and z the ionic charge number. The straight line in Figure 3 is eq 5 with u as a constant. This equation gives a reasonable fit, and it is concluded that the ionic mobilities are nearly the same for the ions studied. These

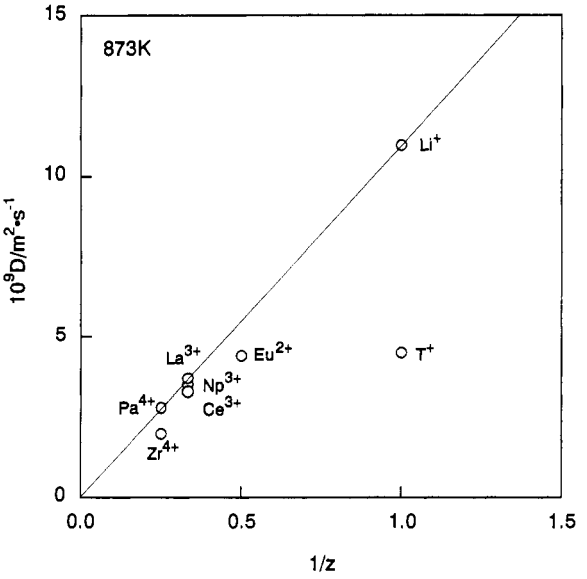

Figure 3. Ionic charge dependence of diffusion coefficients in molten Li_2BeF_4 at 873 K. The diffusion coefficients are taken from the literature for Li^+ (*7*) and T^+ (*8*), and interpolated by eq 4 from the results in Table 1 for others. The line is calculated from eq 5, the Nernst–Einstein equation with a constant ionic mobility.

results are similar to those obtained in aqueous solutions. Although some deviations from the proportionality are observed in Figure 3, for example, for T^+ and Zr^{4+}, they can be interpreted in terms of solvation effects of small ions as observed in aqueous solutions. The ionic radii of T^+ and Zr^{4+} are smaller than those of Li^+ and Pa^{4+}, respectively, and larger interactions of these ions with the solvent constituents such as F^- are expected.

Conclusions

The temperature dependences of the diffusion coefficients of highly charged actinide and lanthanide ions were measured in molten Li_2BeF_4. The observed temperature dependences were compared with the Stokes–Einstein equation. The high diffusion coefficients observed despite the high viscosity were explained by considering the microscopic structure of molten Li_2BeF_4. The ionic charge dependence of the diffusion coefficient was interpreted by the Nernst–Einstein equation. The results were similar to those in aqueous solutions.

Acknowledgment

This work was performed under the Visiting Researchers' program of the Kyoto University Research Reactor Institute. The authors wish to thank Prof. T. Tamai and Mr. S. Nishikawa for their encouragement and Messrs. M. Miyazaki and Y. Asaoka for their assistance.

Literature Cited

(1) Weinberg, A. M.; et al. *Nucl. Appl. Technol.* **1970**, *8*, 105.
(2) Ferris, L. M.; Mailen, J. C.; Lawrance, J. J.; Smith, F. J.; Nogueira, E. D. *J. Inorg. Nucl. Chem.* **1970**, *32*, 2019.
(3) Ferris, L. M.; Mailen, J. C.; Smith, F. J. *J. Inorg. Nucl. Chem.* **1971**, *33*, 1325.
(4) Moriyama, H.; Yajima, K.; Nunogane, N.; Ohmura, T.; Moritani, K.; Oishi, J. *J. Nucl. Sci. Technol.* **1984**, *21*, 949.
(5) Oishi, J.; Moriyama, H.; Moritani, K.; Maeda, S.; Miyazaki, M.; Asaoka, Y. *J. Nucl. Mater.* **1988**, *154*, 163.
(6) Moriyama, H.; Miyazaki, M.; Asaoka, Y.; Moritani, K.; Oishi, J. *J. Nucl. Mater.* **1991**, *182*, 113.
(7) Iwamoto, N.; Tsunawaki, Y.; Umesaki, N.; Ohno, H.; Furukawa, K. *J. Chem. Soc., Faraday Trans.* **1979**, *75*, 1277.
(8) Oishi, J.; Moriyama, H.; Maeda, S.; Asaoka, Y. *Fusion Eng. Des.* **1989**, *8*, 317.
(9) Lamb, H. *Hydrodynamics*; Cambridge University Press: London and New York, 1932; p 604.
(10) Forcheri, S.; Wagner, V. *Z. Naturforsch.* **1967**, *22a*, 1171.
(11) Bockris, J. O'M.; Richards S. R.; Nanis, L. *J. Phys. Chem.* **1965**, *69*, 1627.
(12) Moynihan, C. T. *Ionic Interactions*; Academic Press: New York and London, 1971; Vol. 1, Chapter 5.
(13) Cantor, S.; Ward W. T.; Moynihan, C. T. *J. Chem. Phys.* **1969**, *50*, 2874.
(14) Baes, Jr., C. F. *J. Solid State Chem.* **1970**, *1*, 159.

Received for review May 12, 1993. Accepted September 2, 1993.• This work was partly supported by a Grant-in-Aid for Scientific Research from the Ministry of Education, Science and Culture.

• Abstract published in *Advance ACS Abstracts*, November 15, 1993.